E-Drive SiC MOSFET Inverter with Self Calibrating VON-based Junction Temperature Estimator

E-Drive SiC MOSFET Inverter with Self Calibrating V_{ON}-based Junction Temperature Estimator

Fausto Stella
Department of Energy *Galileo Ferraris*
Politecnico di Torino
Turin, Italy
fausto.stella@polito.it

Paolo Pescetto
Department of Energy *Galileo Ferraris*
Politecnico di Torino
Turin, Italy
paolo.pescetto@polito.it

Gianmario Pellegrino
Department of Energy *Galileo Ferraris*
Politecnico di Torino
Turin, Italy
gianmario.pellegrino@polito.it

***Abstract*— Monitoring junction temperature is of key importance in SiC MOSFET power converters, to guarantee their reliability. A feasible method for estimating the junction temperature of a power MOSFET is to take advantage of the correlation between junction temperature and conduction resistance. However, this approach requires a preliminary calibration of the V_{ON} characteristic as a function of the junction temperature of the device. This is usually performed offline through dedicated laboratory equipment. This work proposes a novel method for measuring the on-voltage versus temperature characteristic directly on the drive, with the motor already connected to the inverter, thus avoiding the necessity of a dedicated test rig. The commissioning procedure starts with a self-heating phase, followed by the R_{ON} measurement stage. A polynomial fit is proposed to extrapolate the R_{ON} characteristic out of the domain of measured temperatures. The obtained data can then be used for online estimation of the junction temperature of the six MOSFETs on board of a PWM operated three-phase inverter.**

Keywords—RON, SiC MOSFET, Junction Temperature Estimation, 3-Phase Inverter.

I. INTRODUCTION

SiC-based power devices have revolutionized power conversion, yielding to new levels of efficiency and power density. Compared to their silicon counterparts, they offer lower switching and conduction losses, lower temperature sensitivity, better thermal conductivity of the die, higher levels of operating temperature and breakdown voltage [1]-[4]. SiC semiconductors are becoming widely used in the automotive and aerospace sectors, where power density represents the major figure of merit. However, to take full advantage of these devices and guarantee the converter reliability, the maximum junction temperature of the power devices must imperatively be limited. Exceeding, even transitory, the maximum junction temperature recommended by the manufacturer can lead in the best-case scenario to the premature ageing of the component and at worst to its immediate failure. To address this problem different techniques may be adopted to measure or to estimate the junction temperature, but few of them are suitable for an industrial or automotive environment. Direct measurement techniques make use of a thermal camera or a thermistor in direct contact with the die. The use of a thermal camera requires removing the insulating encapsulant of the die to provide visual access, and it is therefore a not viable solution for industrial applications.

The **thermistor** in direct contact with the chip is a viable solution, available on the market [5], although guaranteeing the insulation between the thermistor and the die is challenging and the presence of this adds a risk of failure. Furthermore,the non-ideal thermal coupling between the thermistor and the die produces a delayed and attenuated temperature measurement [6].

State of the art power converters combine the measurement of a thermistor monitoring the temperature of the heatsink or the baseplate of the power module with a thermo-electric model of the power device. However, the electrical and thermal models of the power devices are usually unknown or known very roughly [7]-[9]. This inevitably leads to retain large safety margins that are not acceptable in cost critical applications like automotive. Alternatively, several techniques based on Thermo Sensitive Electrical Parameters (TSEPs) have been developed. These techniques enable to estimate the junction temperature by using indirect indicators such as currents and voltages measured across the device. Depending on the semiconductor technology, different TSEPs can be used [10], [11]. However, their use is still limited to a laboratory environment with controlled testing conditions and dedicated equipment. Starting from the well know dependency between the conduction resistance (R_{ON}) of SiC MOSFETs and their junction temperature, new solutions were proposed for real time estimating the junction temperature of the power devices of a 3-phase inverter operating in PWM mode [13]. This TSEP technique is here implemented in a real case scenario. The functional block of the proposed temperature estimator is shown in Fig. 1. The ON voltage and current of each MOSFET are measured at each PWM period during operation and entered into a dedicated temperature lookup table (LUT) $\theta_{j,est}\,(i_{DS}, R_{ON})$. Each device of the bridge has a unique table, obtained with dedicated laboratory equipment like a curve tracer. In [13] the temperature LUT was obtained directly on the converter with a self-calibration test without using any dedicated measurement equipment, with the exception of an hotplate and a three-phase inductive load. *This work proposes an improved self-commissioning test and data manipulation, to obtain the temperature law of each power device with the inverter directly connected to the target motor and without additional equipment.* Respect to [13], the LUTs are replaced by a polynomial fit, for the sake of data extrapolation when out of the domain of identification.

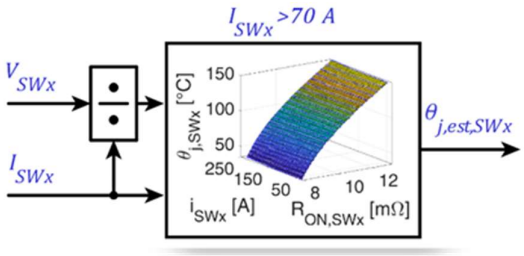

Fig. 1. Online junction temperature estimator functional block.

II. Polynomial Model of the R_{ON} Characteristic

The ON state resistance of the power MOSFETs is a non-linear characteristic without a unique formalized analytical model. In this work, the dependency of R_{ON} with respect to the die temperature θ_j and the conducted current i are considered:

$$R_{ON} = R_{ON}(\theta_j, i) \tag{1}$$

In particular, according to [14], for a fixed current $\hat{R}_{ON}(\theta_j)$ is a quadratic function of the die temperature, while for a fixed temperature $\hat{R}_{ON}(i)$ with a linear function of the current. This leads to the proposed polinomal model:

$$\hat{R}_{ON}(\theta_j, i) = R_0 + k_{\theta 1}\theta_j + k_{\theta 2}\theta_j^2 + k_i i \tag{2}$$

where $\hat{R}_{on}$ stands for estimated ON resistance, intending that the model will be used also for extrapolation out of the domain of identification.

The validity of the polynomial representation in (2) is verified based on the data collected in [13], where the same inverter adopted for this work was tested using a commissioning procedure similar to the one proposed here. In [13], the 6 inverter MOSFETs were individually characterized in their full operating region, with a maximum temperature of 150°C and a maximum current of 240 A. The measured data were then interpolated based on (2). The results are reported in Fig. 2 and Fig. 3, comparing the measured data with the fitted analytical surface. As can be noticed, the correspondence between the model and the measured data is good in the full operating domain, with a Root Mean Square Error (RMSE) lower than 0.55% and a maximum discrepancy lower than 1.3% for all MOSFETs.

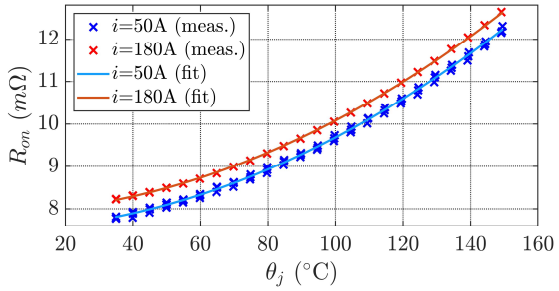

Fig. 2. Measured and interpolated $R_{ON}(\theta_j, i)$ characteristic for one of the 6 inverter MOSFETs. R_{ON} characteristic measured for a phase current of 50 and 180 A based on [13] ("x" points) and interpolated using (2).

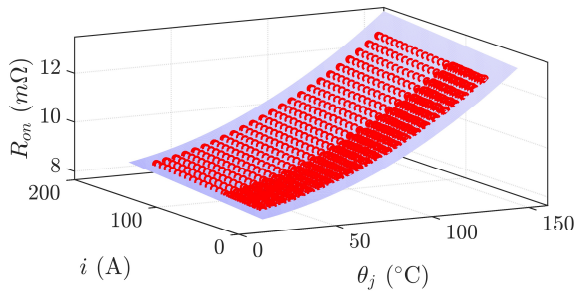

Fig. 3. $R_{ON}(\theta_j, i)$ characteristic measured as in [13] (red points) and interpolated based on (2) (blue surface).

III. Description of the Set-Up

A. 3-phase SiC VSI

The prototypal three-phase inverter used to validate the proposed technique is shown in Fig. 4. It consists of three half-bridges SiC MOSFETs power modules BSM180d12p3c007 by ROHM, whose power ratings are listed in Table I. Each power module embeds two SiC MOSFETs and two antiparallel SiC diodes. On top of the power converter, the control board embeds a STM32H7 MCU, a SPARTAN6 FPGA, three phase current sensors, CAN communication, encoder interface and so on. The converter was developed for a race car designed for the formula SAE electric students competition, therefore it embeds all the hardware to operate on a car. The power section schematic of the converter is shown in Fig. 5, where the sampled quantities are reported in red. Besides the measurements of the DC bus voltage, phase currents and heatsink temperature, which are common to three-phase inverters for motor drive application, the conduction voltage of each switch is additionally measured.

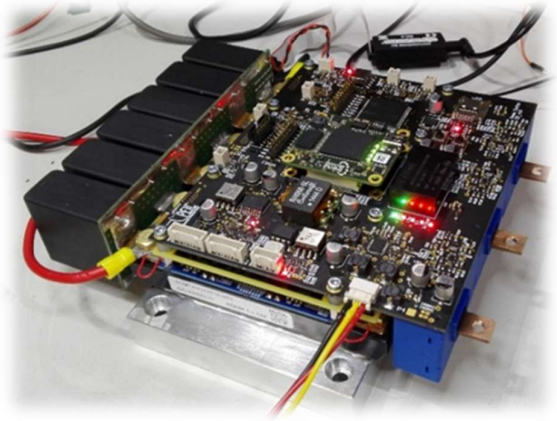

Fig. 4. Prototypal three-phase SiC inverter.

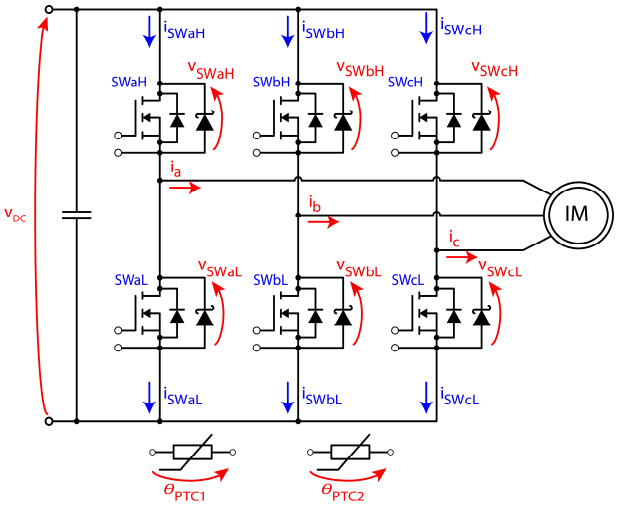

Fig. 5. Power section schematic, with sampled quantities in evidence.

TABLE I. POWER MODULE
ROHM BSM180D12P3C007

Rated current (θ_{case}=60°C)	180 A
Breakdown voltage	1200 V
R_{ON} @ 25°C,180A	10 $m\Omega$
Max Junction Temperature	175 °C

B. Induction Motor

To validate the proposed technique, the three phase-inverter was connected to the induction motor (IM), shown in Fig. 6, whose power ratings are shown in Table II. This is a low-voltage high-current motor that was selected for validation of the temperature estimate at high current. A reduced DC-link voltage of 200 V was used in the tests, accordingly.

Fig. 6. Automotive inductor motor used for the tests.

TABLE II. INDUCTION MOTOR RATINGS

Rated power	10 kW
Rated frequency	200 Hz
Rated phase current	124 Arms
Rated torque	50 Nm
Rated voltage	70 V

IV. PROPOSED SELF-CALIBRATION TEST

The online junction temperature estimation requires the preliminary calibration stage of the six θ_j (i_{DS}, R_{ON}) LUTs, one per SiC MOSFET. The calibration test is performed automatically with the inverter connected to the motor, and does not require user intervention or change of connections respect to the normal operation of the drive. Moreover, it does not produce relevant movement of the shaft, and it can be executed independently by the load being mechanically connected or not to the motor. As visible from Fig. 6, the tests were performed at free shaft, which is the worst case scenario in this sense.

Normally, the calibration procedure is executed once at the beginning of the life of the drive and the six LUTs are stored in the controller memory. As said, the procedure may be repeated for an update of R_{ON} after partial aging of for diagnostic and prognostic purposes [12].

The test consists of: 1) preliminary heating, 2) sequence of current pulses and 3) fit of the R_{ON} characteristics.

1. Preliminary Heating

In this phase, the converter heatsink is heated to 85°C imposing to the induction motor a rotating 80 Apk current vector, with the inverter's liquid cooling system turned off. The rotating current vector (set of three-phase sinusoidal currents at 100Hz) distributes the conduction and switching losses evenly between the MOSFETs, whereas the frequency of 100 Hz avoids the generation of continuous torque at the shaft. Moreover, the direction of rotation of the current vector is reversed every time a significant movement is detected using the motor encoder as shown in Fig. 7, to further avoid relevant rotor movement. The rotating current amplitude is sufficient to heat the heatsink to the target temperature in reasonable time without risk of exceeding the recommended maximum junction temperature. The heating phase is stopped once the heatsink thermistor reaches 85°C, and the heatsink starts a slowl natural cooling.

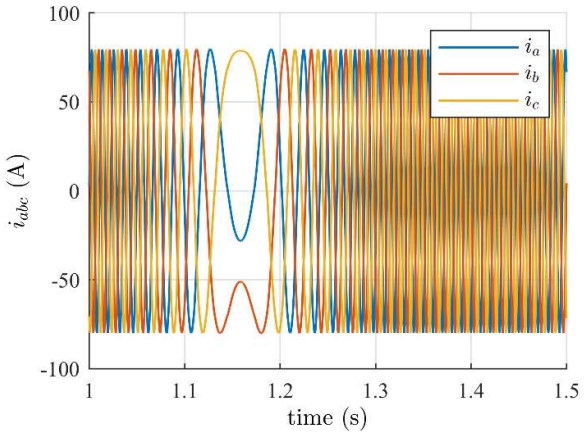

Fig. 7. Heating sinusoidal current (80Apk, 100Hz). Every time a rotor movement is detected, the 3-phase sequence is reversed.

2. Sequence of current pulses

The temperature LUTs of the six MOSFETs are measured using the current-pulse based procedure of [13]. The key steps are:

1. The heatsink ispreliminarily heated at 85°C as said, and cools down slowly. With the phase currents turned off,

the prerequisite condition of the junction temperature being equal to the heatsink temperature is re-established within a few minutes.

2. When the temperature of the heatsink reaches 80°C a first set of short current pulses (150 µs circa) of growing amplitude (from 5 to 150 A) is commanded by the converter along each of the six inverter axes (Fig. 8 -Fig. 11). For each pulse, the currents and the voltages across the six switches are stored together with the measured heatsink temperature.
3. The sequence of pulses is repeated when the heatsink temperature measured by the thermistor drops of another 2.5°C and so on (Fig. 12).
4. When the temperature of the heatsink approaches the room temperature (e.g. 35°C), the identification is terminated.

The main assumption behind this approach is that during this stage, the temperature of the heatsink measured with the thermistor equals the temperature of the junction. This is justified by the short duration of the current pulses (150 µs) and to the slow natural cooling (total cooling time is around 90 minutes). As shown in previous work [13], the temperature rise due to a single current pulse is below 2°C. Furthermore, the idle time of 200 ms between consecutive pulses make the pulses thermally independent between one another.

Respect to [13], the range of characterization is reduced here from 150°C to 80°C and from from 240A to 150A. Temperature wise, the inverter coolant must not reach its boiling temperature. Moreover, it should be remarked that the heatsink is heated using the MOSFETs losses whose junction temperature must be higher than the temperature of the heatsink, thus allowing the heat transfer and the power devices. Therefore, the feasible heatsink temperature must be kept sufficiently lower than the maximum operating temperature of the MOSFETs.

Dealing with the 150 A range, this relates to the slew-rate current limitations imposed by the machine inductance and by the available DC-link voltage. Otherwise said, due to the machine inductance and to the available DC-link voltage, it is not possible to reach the target current of 240 A without increasing the pulse duration. Such limitations are expected when the test is performed directly on the drive and not in the lab, with selected load inductors.

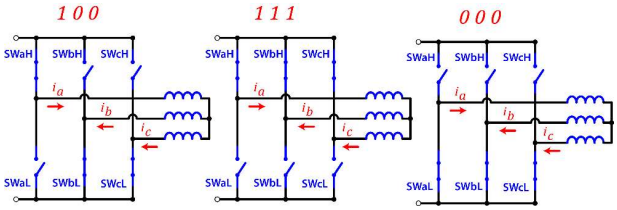

Fig. 8. Inverter switches configurations and phase currents during the commissionig alog a+ axis.

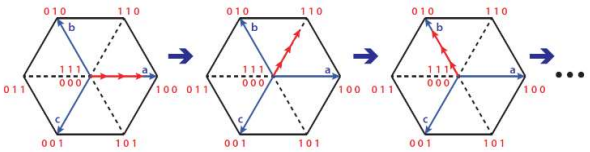

Fig. 9. Current pulses along the six inverter axes.

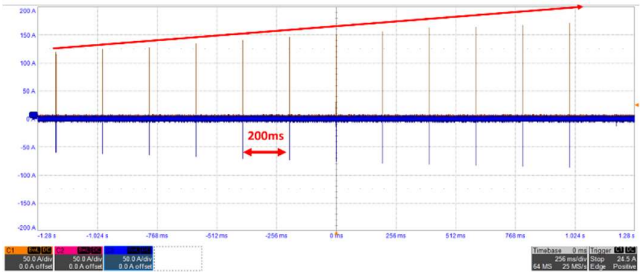

Fig. 10. Current pulses of increasing amplitude along the a + axes spaced by 200 ms.

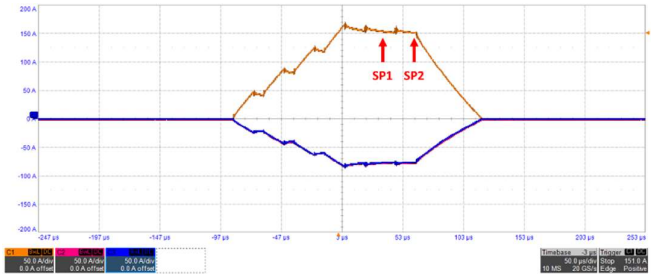

Fig. 11. Detail of the single pulse showing the sampling time SP1 (high side switches) and SP2 (low side switches).

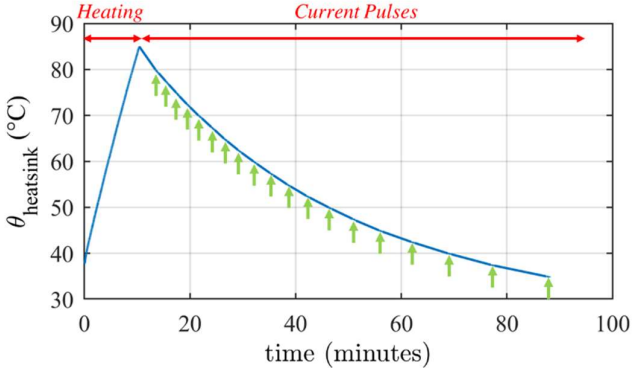

Fig. 12. Heatsink temperature during the Heating and Current pulses injection phases. In correspondance of each green arrow a set of current pulses of growing amplitude is imposed along the six inverter axis, thus mapping all the six inverter MOSFETs.

3. *Extralpolation of R_{ON} characteristics*

Upon data collection, the ON resistance versus die temperature and drain current characteristic is fitted using the polynomial function (2). The Linear Least Square (LLS) [15] regression algorithm is adopted to retrieve the optimal set of coefficients $R_0, k_{\theta 1}$, $k_{\theta 2}$ and k_i. This error minimization algorithm can be implemented in industrial microcontrollers without significant hardware requirements.

The R_{ON} characteristics measured in [13] in the full operating region 150°C, 240 A is used as reference. The interpolation of the data with the analytical model (2) permits to extrapolate the $\hat{R}_{ON}(\theta, i)$ characteristic out of the measurement domain, to cover the full operating region. The results of the LLS fit and extrapolation are reported in Fig. 13 and Fig. 14.

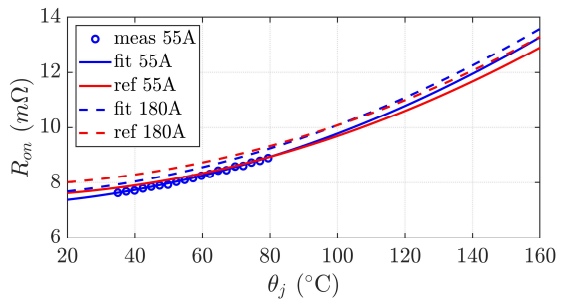

Fig. 13. Result of the LLS fit based on the self-commissioning data for one of the inverter MOSFETs. Red lines: reference characteristic for 55 A and 180 A; blue dots: measured data at 55 A; blue lines: polynomial estimates at 55 A and 180 A.

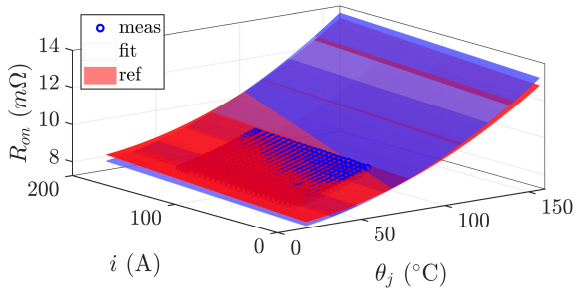

Fig. 14. Comparison between the reference characteristic (red) and the extrapolated surface (blue) based on the proposed commissioning. The blue dots are the measured points.

The adopted analytical model (2) is physically reasonable [14] and easily solved by LLS also on board of the drive, as said. Once the $\hat{R}_{ON}(\theta_j, i)$ fit is done, the inverse function, $\hat{\theta}_j(R_{on}, i)$ can be conveniently evaluated:

$$\hat{\theta}_j(R_{on}, i) = \frac{-k_{\theta 1} + \sqrt{k_{\theta 1}^2 - 4k_{\theta 2}(k_i i + R_0 - R_{on})}}{2k_{\theta 2}} \qquad (3)$$

This equation can be used for direct temperature estimate or for building 2-dimensional LUTs $\hat{\theta}_j(R_{on}, i)$.

V. Parameter Dispersion

As mentioned, the commissioning procedure analyzes the R_{ON} characteristic of each of the power device. This puts in evidence the parametric dispersion between different exemplars of the same component. The discrepancy is mostly due to min-max tolerance of the power devices resistance and partly to non-idealities of the inverter sensors.

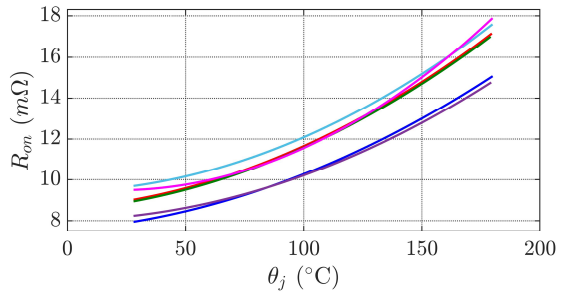

Fig. 15. R_{ON} characteristic of the 6 inverter MOSFETs at 180 A.

The necessity of adopting a dedicated characteristic for each MOSFET is demonstrated in Fig. 15, where the R_{ON} at 180 A characteristics of the devices are reported.

VI. Experimental Results

The $\hat{R}_{ON}$ characteristics measured and extrapolated with the proposed method were compared with the reference maps of [13], showing a negligible discrepancy when the current in the device is relevant. At low current, the discrepancy is slightly higher due to the difficulty of correctly measuring R_{ON}. Anyway, the temperature estimation error is still acceptable. Furthermore, this condition is not critical in terms of junction temperature, as the current in the device is low. The comparison of the two characteristics is reported in Fig. 16 and Fig. 17, where a 1 Hz, 220 Apk rotating current vector was imposed to the IM.

The temperature of the six power MOSFETs cannot be estimated for $i_{DS} < 0$ due to the presence of the antiparallel diodes. When $i_{DS} < 0$ the current sharing between the diode and the MOSFET is unknown. Nevertheless, the negative current case is not critical temperature wise for two reasons:

1. Part of the current is conducted by the diode.
2. When $i_{DS} < 0$ the MOSFET has a soft turn-on, and therefore the commutation losses tend to zero.

Furthermore at low currents below 70 A the junction temperature is not estimated as it is not possible to precisely measure V_{ON} due to the poor signal to noise ratio (the amplitude of the noise became comparable with the amplitude of the signal).

As can be noticed from Fig. 17, the maximum temperature estimation error between the reference data and the proposed method is in the range of 5°C, which is considered acceptable for the considered application.

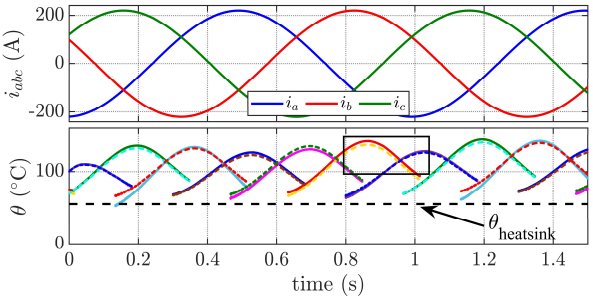

Fig. 16. Online juntion temperature estimation of the 6 MOSFETs using the reference LUTs (solid lines) and the extrapolated characteristic based on the proposed commissioning (dashed lines).

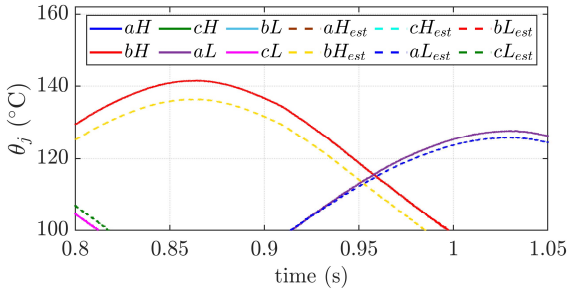

Fig. 17. Detail of Fig. 16.

VII. CONCLUSIONS

A. Considerations

A new procedure for the direct commissioning of ON-resistance based temperature monitoring of SiC MOSFETs is proposed and experimentally validated. Compared to the literature, it is now possible to perform the calibration process with the inverter connected to the AC motor, without any specialized equipment out of the drive itself. The only additional feature respect to a standard voltage-source inverter is the V_{ON} measurement system that can be eventually integrated in the in the gate driver circuitry at a reduced additional complication. Furthermore, during the commissioning stage the cooling system must be interrupted/deviated for permitting a fast temperature rise.

In previous work [13] the calibration test was performed by connecting the inverter to a three-phase inductor and the heatsink was externally heated up to 150 °C, while injecting current pulses up to 240 A (maximum operational current of the converter). In this work, data are collected in a reduced temperature and current range and the semiconductors maps are extrapolated to cover the full operational domain using a suitable polynomial fit. The experimental results show that the extrapolated LUTs are sufficiently accurate to guarantee a temperature estimation with an error below 5°C in each of the 6 MOSFETs of the bridge under real operating conditions. Additional errors may be possible due to measurement noise and uncertainties; however the proposed approach is way more precise and reliable compared to most of junction temperature estimation techniques currently used in industry and in automotive.

The temperature estimate can be used to actively limit the temperature of the switches, so to fully exploit the safe operating area of the semiconductors virtually without any risk of failure. The extension of the proposed technique to drives adopting different types of motors and its validation on a wide range of power modules from different manufacturers are currently ongoing. The risk of demagnetization must be taken into account when dealing with Permanent Magnet motors.

B. Prospect Applications

The proposed technique is particularly suitable for all the fields where high performance and/or reliability are essential like aerospace, automotive, military and medical. Despite the additional cost introduced by the V_{ON} measurement system, overall cost reduction is expected thanks to a better exploitation of the SOA, besides the improved reliability.

C. Ageing

It is well known from the literature that semiconductors resistance increases over time with the aging of the component. This is due to multiple reasons like wire bonding lift-off, die delamination and so on [16], [17]. As the proposed methodology is based on the R_{ON} measurement, a rise in its value would cause the junction temperature to be overestimated. Depending on the component package, manufacturing technology and aging methodology the increase of R_{ON} over the time can be more or less severe. The proposed calibration procedure can be repeated from time to time to asses ageing. E.g. every 1000 hours of use for and electric vehicle. The process can be fully automated and performed while the vehicle is recharging. The R_{ON} measurement can be used as an indirect indicator of the health state of the component. This was done in a previous work [18], where the R_{ON} was used for prognostic purposes.

REFERENCES

[1] ROHM Semiconductors application note: "SiC Power Devices and Modules".

[2] Bob Callanan. “Application Considerations for Silicon Carbide MOSFETs”. Cree. Jan. 2011.

[3] J. W. Palmour, “Silicon carbide power device development for industrial markets,” in 2014 IEEE International Electron Devices Meeting, Dec. 2014.

[4] L. Zhang et Al. “Performance Evaluation of High-Power SiC MOSFET Modules in Comparison to Si IGBT Modules,” IEEE Transactions on Power Electronics, Feb. 2019.

[5] Infineon, FF400R07A01E3_S6 Datasheet, April 2020. Available: https://www.infineon.com/dgdl/Infineon-FF400R07A01E3_S6-DataSheet-v03_04-EN.pdf?fileId=5546d46262b31d2e016301931a14339a

[6] F. Stella, G. Pellegrino, E. Armando, and D. Daprà, “Online Junction Temperature Estimation of SiC Power MOSFETs Through On-State Voltage Mapping,” IEEE Transactions on Industry Applications, vol. 54, no. 4, pp. 3453–3462, Jul. 2018, doi: 10.1109/TIA.2018.2812710.

[7] P. Liu, X. Zhang, S. Yin, C. Tu, and S. Huang, “Simplified Junction Temperature Estimation using Integrated NTC Sensor for SiC Modules,” in 2018 IEEE International Power Electronics and Application Conference and Exposition (PEAC), Nov. 2018.

[8] M. H. M. Sathik et al., “Online electro-thermal model for real time junction temperature estimation for insulated gate bipolar transistor (IGBT),” in 2016 IEEE 2nd Annual Southern Power Electronics Conference (SPEC), Dec. 2016.

[9] C. Sintamarean, F. Blaabjerg, and H. Wang, “A novel electro-thermal model for wide bandgap semiconductor based devices,” in 2013 15th European Conference on Power Electronics and Applications (EPE), Sep. 2013.

[10] D. L. Blackburn, “Temperature measurements of semiconductor devices - a review,” in Twentieth Annual IEEE Semiconductor Thermal Measurement and Management Symposium, 2004.

[11] Y. Avenas et Al., “Temperature Measurement of Power Semiconductor Devices by Thermo-Sensitive Electrical Parameters—A Review,” IEEE Transactions on Power Electronics, Jun. 2012.

[12] H. Luo, F. Iannuzzo, F. Blaabjerg, M. Turnaturi, and E. Mattiuzzo, “Aging precursors and degradation effects of SiC-MOSFET modules under highly accelerated power cycling conditions,” in 2017 IEEE Energy Conversion Congress and Exposition (ECCE), Oct. 2017, pp. 2506–2511. doi: 10.1109/ECCE.2017.8096478.

[13] F. Stella, G. Pellegrino, and E. Armando, “Three-phase SiC inverter with active limitation of all MOSFETs junction temperature,” Microelectronics Reliability, Jul. 2020.

[14] B. J. Baliga, Fundamentals of Power Semiconductor Devices. Springer US, 2008.

[15] T. Söderström and P. Stoica, *“System Identification”*. Hemel Hempstead, U.K.: Prentice-Hall, 1989.

[16] S. Yang, D. Xiang, A. Bryant, P. Mawby, L. Ran, and P. Tavner, “Condition Monitoring for Device Reliability in Power Electronic Converters: A Review,” IEEE Transactions on Power Electronics, vol. 25, no. 11, pp. 2734–2752, Nov. 2010, doi: 10.1109/TPEL.2010.2049377.

[17] H. Wang, M. Liserre, and F. Blaabjerg, “Toward Reliable Power Electronics: Challenges, Design Tools, and Opportunities,” IEEE Industrial Electronics Magazine, vol. 7, no. 2, pp. 17–26, Jun. 2013, doi: 10.1109/MIE.2013.2252958.

[18] F. Stella, G. Pellegrino, and E. Armando, “Coordinated On-line Junction Temperature Estimation and Prognostic of SiC Power Modules,” in 2018 IEEE Energy Conversion Congress and Exposition (ECCE), Sep. 2018, pp. 1907–1913. doi: 10.1109/ECCE.2018.8557850.